Metabolite diffusion up to very high b in the mouse brain in vivo: Revisiting the potential correlation between relaxation and diffusion properties

Clémence Ligneul, Marco Palombo, Julien Valette

FULL PAPER

Magnetic Resonance in Medicine 00:00–00 (2016)

Metabolite Diffusion up to Very High *b* in the Mouse Brain In Vivo: Revisiting the Potential Correlation between Relaxation and Diffusion Properties

Clémence Ligneul,[1,2] Marco Palombo,[1,2] and Julien Valette[1,2]*

Purpose: To assess the potential correlation between metabolites diffusion and relaxation in the mouse brain, which is of importance for interpreting and modeling metabolite diffusion based on pure geometry, irrespective of relaxation properties (multicompartmental relaxation or surface relaxivity).

Methods: A new diffusion-weighted magnetic resonance spectroscopy sequence is introduced, dubbed "STE-LASER," which presents several nice properties, in particular the absence of cross-terms with selection gradients and a very clean localization. Metabolite diffusion is then measured in a large voxel in the mouse brain at 11.7 Tesla using a cryoprobe, resulting in excellent signal-to-noise ratio, up to very high *b*-values under different echo time, mixing time, and diffusion time combinations.

Results: Our results suggest that the correlation between relaxation and diffusion properties is extremely small or even nonexistent for metabolites in the mouse brain.

Conclusion: The present work strongly supports the interpretation and modeling of metabolite diffusion primarily based on geometry, irrespective of relaxation properties, at least under current experimental conditions. **Magn Reson Med 000:000–000, 2016.**

Key words: magnetic resonance spectroscopy; metabolite; diffusion; relaxation; brain

INTRODUCTION

The diffusion of brain endogenous metabolites, as measured by diffusion-weighted MR spectroscopy (DW-MRS), has the enormous potential to yield specific information about the intracellular environment, due to the cell-specific compartmentation of most metabolites (for review, see Nicolay et al) (1). In recent works, we and others have interpreted and modeled brain metabolite diffusion in vivo in terms of cell microstructure/geometry (2–7), as also usually done for water diffusion. This is assuming that diffusion attenuation mainly results from the geometry, irrespective of the potential correlation that might exist between relaxation time and diffusion. Such correlation may of course arise from the presence of different compartments, each with their own relaxation times and diffusion properties (e.g., cytosolic versus mitochondrial compartments). If only a single compartment exists, correlation between relaxation and measured diffusion can still arise from surface (or wall) relaxivity, i.e., where each interaction of a metabolite with a cellular membrane leads to a quicker relaxation [this has been recognized for a long time in NMR of porous media (8,9)]. A few works have reported a dependency of brain metabolite signal attenuation on the echo time, suggesting that such a correlation might exist and be significant (10–12), as also reported for water (13,14). It is thus legitimate to question the validity of interpreting and modeling intracellular metabolite diffusion based on pure geometry, irrespective of relaxation properties.

Here, we propose to revisit the potential relation between metabolite diffusion and relaxation by taking advantage of new methodological features. First, a new sequence is introduced, which presents several nice properties, in particular the absence of cross-terms with selection gradients (resulting in the possibility to modify sequence timing without any bias resulting from variations in cross-terms) and a very clean localization. Metabolite diffusion is then measured in a large voxel in the mouse brain at 11.7 Tesla (T) using a cryoprobe, resulting in excellent signal-to-noise ratio (SNR). Using this setup, we measure metabolite diffusion up to very high *b*-values under different echo time (TE), mixing time (TM), and diffusion time (Δ) combinations. Our results suggest that, under these experimental conditions, the correlation between relaxation and diffusion properties is extremely small or even nonexistent.

[1]Commissariat à l'Energie Atomique et aux Energies Alternatives (CEA), Direction des Sciences du Vivant (DSV), Institut d'Imagerie Biomédicale (I2BM), MIRCen, Fontenay-aux-Roses, France.

[2]Centre National de la Recherche Scientifique (CNRS), Université Paris-Sud, Université Paris-Saclay, UMR 9199, Neurodegenerative Diseases Laboratory, Fontenay-aux-Roses, France.

Grant sponsor: the European Research Council; Grant number: "INCELL" project, ERC grant 336331.

*Correspondence to: Julien Valette, Commissariat à l'Energie Atomique et aux Energies Alternatives (CEA), Bâtiment 61, 8 Route du Panorama, 92260 Fontenay-aux-Roses, France. E-mail: julien.valette@cea.fr

Received 17 November 2015; revised 26 January 2016; accepted 23 February 2016

DOI 10.1002/mrm.26217

Published online 00 Month 2016 in Wiley Online Library (wileyonlinelibrary.com).

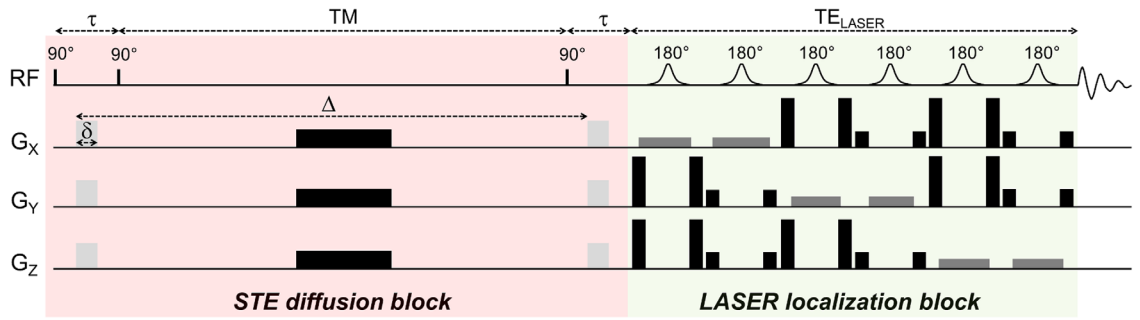

FIG. 1. Outline of the diffusion-weighted STE-LASER sequence. The sequence starts by an STE block, where the 90° are achieved by nonselective 100-μs hard pulses. The STE block includes diffusion-weighting gradients (light gray) of duration δ and separated by Δ. These diffusion gradients are also used as spoilers to ensure that, when combined with the spoiler inserted during the mixing time (in black), only the stimulated echo is preserved at the end of the block. The sequence is then continued by a LASER localization block, just before acquisition. Because they are isolated from each other (diffusion gradients moment is zero when the LASER block starts), there is no cross-term between diffusion gradients and selection gradients. Total $TE = 2\tau + TE_{LASER}$.

METHODS

DW-MRS Sequence

Cross-terms, which arise from the integral of the product of diffusion gradients' moment with other gradients' moment, result in variations of the effective amplitude and direction of diffusion-weighting, compared with the nominal diffusion-weighing computed based solely on diffusion gradients. Although cross-terms can be taken into account by exact calculation of the whole *b*-matrix, this can be quite tedious, and the situation remains complex in an anisotropic medium because, due to cross-terms, diffusion will not be measured along exactly the same directions when the diffusion gradient amplitude or timing vary. Using a cross-term free sequence would allow being sure to get rid of this potential source of bias.

To intrinsically avoid cross-terms between diffusion gradients and selection gradients, we propose to build a sequence following the approach recently proposed by Shemesh et al (15), i.e., by separating the diffusion module from the localization module. However, unlike in Shemesh et al (15), here the diffusion module consists in a stimulated echo (STE) block performed with nonselective hard pulses. Although this does not provide relaxation-enhancement, it allows reaching much shorter echo times and observing more metabolites, including J-coupled ones, and in the meantime reaching very high diffusion-weighting *b* or very long diffusion time Δ (note that in this study we will consider that gradient duration δ is short compared with gradient separation Δ, so we will assimilate the diffusion time Δ-$\delta/3$ to Δ, although for b calculation the actual Δ-$\delta/3$ value is used). We will write the duration of the STE echo time as 2τ, τ being the time between the centers of the first two 90° pulses.

Spoiling during the TE of the STE block is performed by the diffusion gradients (which, therefore, must always be kept higher than a minimal value, resulting in a minimal *b*-value). During the TM, a long spoiler is inserted, which does not contribute to diffusion-weighting or cross-terms. The localization module coming just after the diffusion module is a LASER ("Localization by Adiabatic SElective Refocusing") block consisting in a train of six adiabatic full passage pulses with adequate slice selection and spoiler gradients (16). Because the diffusion gradient moment at the end of the STE block has been brought back to zero, there is no cross-term with the gradients of the localization module. The LASER gradients have a small contribution to diffusion-weighting, but this contribution is totally independent of the STE module and is, therefore, constant whatever the diffusion gradient strength or the STE timing. The total TE is of course increased and is $TE = 2\tau + TE_{LASER}$. This "STE-LASER" sequence is represented on Figure 1.

Using this sequence, it is straightforward to increase Δ by increasing TM. We can also change τ and TM while keeping Δ constant, as illustrated on Figure 2. Starting from a combination of values $\tau = \tau 1$ and TM = TM1 as illustrated on Figure 2A, one can increase τ (and consequently TE) to $\tau = \tau 2$ without changing TM and Δ, by simply increasing the delay between the first 90° pulse and the first diffusion gradient lobe, and symmetrically the delay between the second diffusion gradient lobe

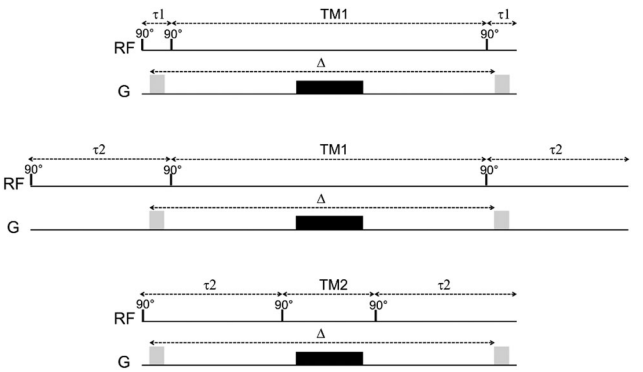

FIG. 2. TE and TM can be varied in the STE block without affecting the diffusion gradients. For simplicity, only one gradient axis is represented, and the LASER block following the STE block is not shown (keeping in mind that it remains unchanged in all situations). From a situation $\tau = \tau 1$ and TM = TM1 (top), the echo time is increased by increasing τ to $\tau 2$ by inserting dead times *outside* the diffusion gradient pair, which leaves TM and Δ unchanged (middle). Then, keeping $\tau = \tau 2$, TM can be reduced down to TM2 = TM1-2 × ($\tau 2$-$\tau 1$) by now inserting dead times *between* the diffusion gradient lobes (but still during the echo time), and reducing TM accordingly to keep Δ unchanged (bottom).

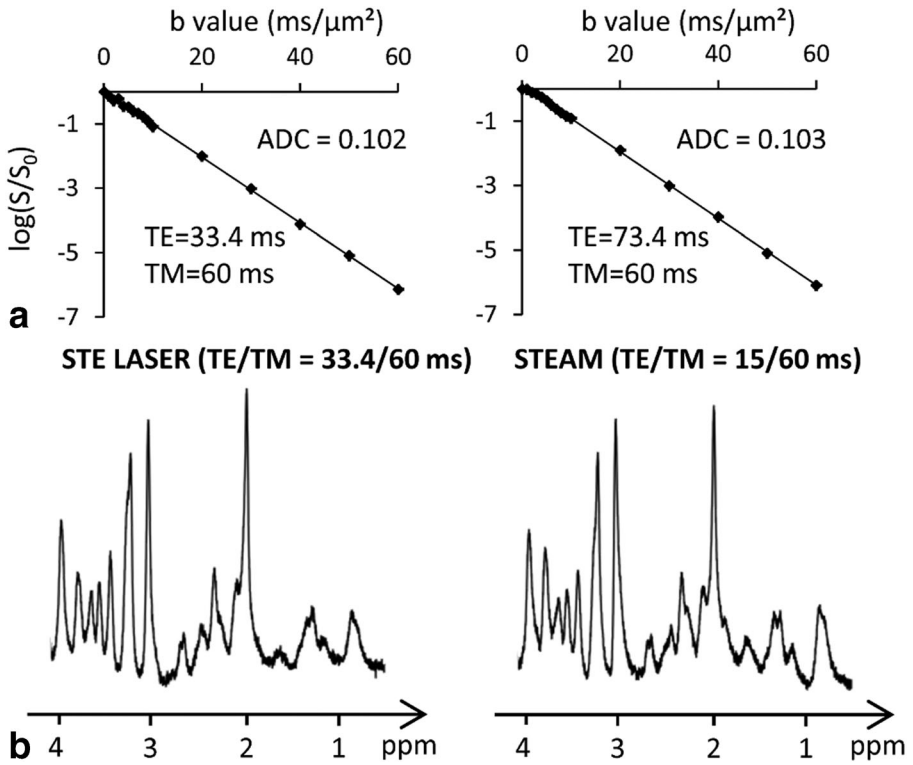

FIG. 3. Validation of sequence performance. **A**: It was first verified that the logarithm of signal attenuation for ethylene glycol was linear up the highest *b*, and resulted in the same free diffusivity in all timing conditions, as exemplified here for acquisitions at two different TE. **B**: It was also verified that the STE-LASER sequence yielded similar spectral quality in vivo compared with a STEAM sequence (TE = 15 ms).

and the LASER block (Fig. 2B). It is then possible to decrease the TM value to TM = TM2 while keeping τ (consequently TE) and Δ constant, by now moving the extra echo time after the first gradient lobe and before the second gradient lobe and reducing TM accordingly (Fig. 2C). While τ and TM are changed, the diffusion gradients are kept absolutely unchanged.

NMR Setup and Experiments

Experiments were performed on a horizontal 11.7 T Bruker scanner running with Paravision 6.0 (Bruker, Ettlingen, Germany). The maximal gradient strength is $G_{max} = 752$ mT/m on each axis, with 100-μs rise time. A quadrature surface cryoprobe (Bruker, Ettlingen, Germany) was used for radiofrequency transmission and reception.

All experimental procedures were approved by the local Ethics Committee (committee #44, approval #10-057). Experiments were performed on 10 male C57BL/6 mice (weight, 28–30 g). Animals were maintained on a stereotaxic bed with a bite and two ear bars. They were anesthetized with 1.2–1.5% isoflurane in a 1:1 mixture of air and dioxygen (1 L/min total flow rate). Mice temperature was monitored with an endorectal probe and maintained at 37°C with regulated water flow, and respiratory rate was continuously monitored using PC SAM software (Small Animal Instruments, Inc., Stony Brook, NY) during scanning.

Spectroscopic signal (5000 Hz spectral width, with 4096 complex data points sampled) was acquired in a large 6.0 × 2.4 × 5.0 mm^3 voxel using the STE-LASER sequence introduced in the previous section. Water suppression was achieved by a VAPOR module. The STE block consisted in three 100-μs hard pulse. The hyperbolic secant pulses used for refocusing in LASER had a 2-ms duration (corresponding to 10 kHz bandwidth). Total duration of the LASER module was $TE_{LASER} = 25$ ms, and the diffusion-weighting corresponding to the LASER block [considering that refocusing occurs at the middle of the RF pulses, i.e., at the middle of the volume of interest (17,18)] was $b_{LASER} = 0.22$ ms/μm^2, which is negligible and will, therefore, not be considered in the rest of the article.

The different combinations that were tested were $\Delta = 64.2$ ms with three different TE/TM combinations (33.4/60 ms, 73.4/60 ms, and 73.4/20 ms) and $\Delta = 254.2$ ms with the three equivalent combinations (33.4/250 ms, 73.4/250 ms, and 73.4/210 ms). Gradient duration δ was 3 ms in all conditions. A minimal gradient strength of 19 mT/m was found to achieve good spoiling for stimulated selection, corresponding to minimal *b*-value of 0.05 ms/μm^2 at $\Delta = 64.2$ ms and 0.15 ms/μm^2 at $\Delta = 254.2$ ms. For each timing combination, the maximal *b*-value was identified as the largest *b*-value still allowing individual scan phasing using metabolite signal (i.e., lowest SNR for NAA on a single scan of ~5 with a line broadening of 3 Hz). This criterion gave us the possibility to go up to $b = 60$ ms/μm^2 (or equivalently 60,000 s/mm^2 in more usual units) for the short TE acquisitions at the two different Δ (each dataset consisted in 16 acquisitions at $b = 0.05$, 1, 2, 3, 4, 5, 6, 7, 8, 9, 10, 20, 30, 40, 50, 60 ms/μm^2). For TE/TM/Δ = 73.4/60/64.2 and 73.4/20/64.2 ms, each dataset consisted in 14 acquisitions between $b = 0.05$ and 40 ms/μm^2, and for TE/TM/Δ = 73.4/250/254.2 and 73.4/210/254.2 ms, each dataset consisted in 13 acquisitions between $b = 0.15$ and 30 ms/μm^2. The number of averages was 128 for each *b*-value. For each timing, an experimental macromolecule (MM) spectrum was acquired in one mouse (512 averages) using the metabolite nulling technique combined with diffusion-

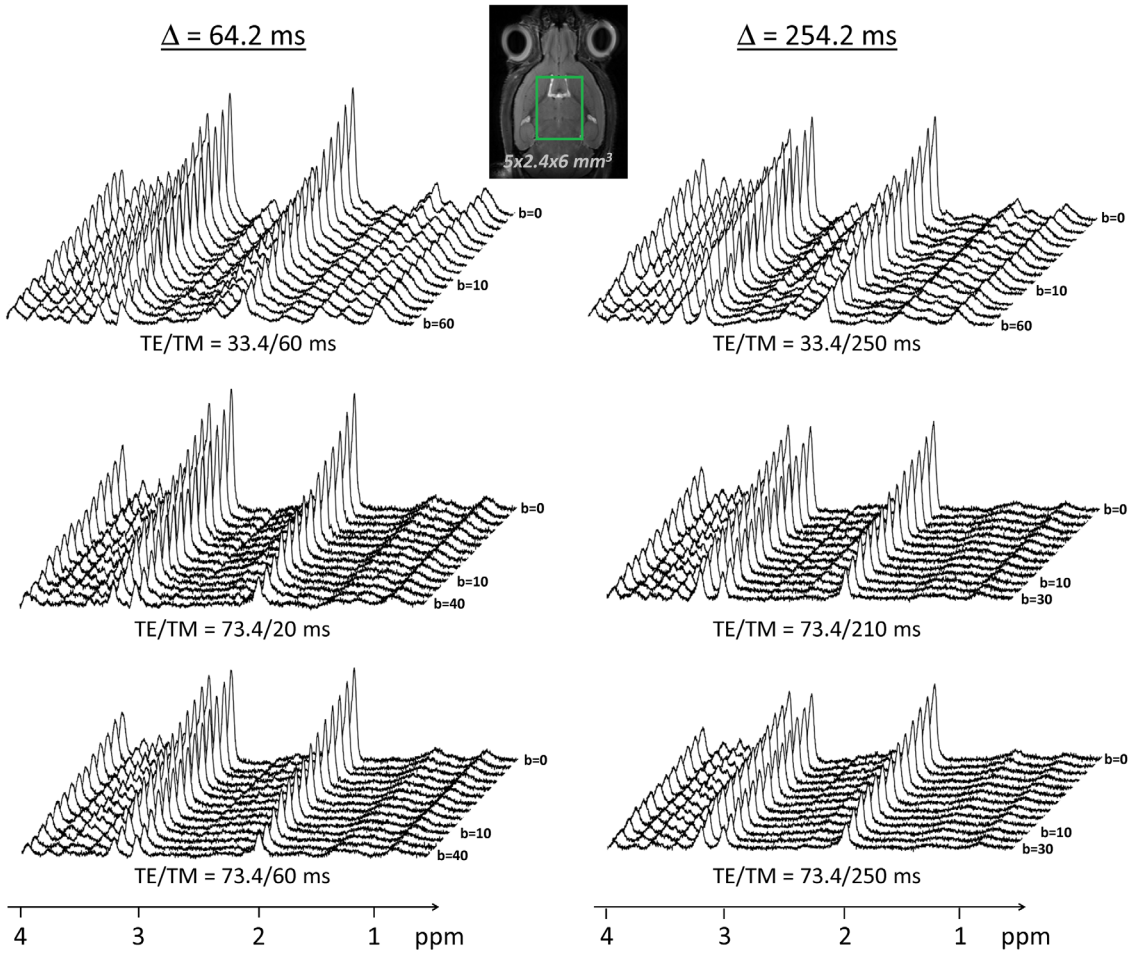

FIG. 4. Typical stack plots of spectra acquired for each TE/TM combination for the two different diffusion times. Each stack plot shown here is acquired in a single experimental session, in a large 5 × 2.4 × 6 mm^3 voxel in the mouse brain. For simplicity the lowest *b*-value was noted "$b = 0$", while it is actually slightly higher (see text for details). Note the excellent SNR (no line broadening was applied).

weighting ($b = 10$ ms/μm^2) to yield cleaner metabolite signal cancellation (19).

The sequence was first validated on an ethylene glycol phantom. Because ethylene glycol has a very high viscosity, signal remains visible even at very high diffusion weighting, which is not the case for water. We could verify that attenuation remained monoexponential up to $b = 60$ ms/μm^2, and yielded the same diffusion coefficient (0.102–0.105 μm^2/ms) for all timing conditions (e.g., see Figure 3A for the signal attenuation at two different TE). We also checked that the STE-LASER sequence (at minimal TE = 33.4 ms) yielded similar SNR in vivo compared with a more conventional STEAM sequence modified for diffusion-weighting (with a minimal TE of 15 ms) (e.g., as used in Pfeuffer et al) (20). This was indeed the case (Fig. 3B), showing that the extra number of radiofrequency pulses used in STE-LASER does not come at the expense of SNR. Hence, the STE-LASER sequence offers adequate performances in terms of sensitivity and diffusion-weighting.

Postprocessing and Data Analysis

Scan-to-scan phase correction was performed on metabolite signal before summing individual scans on Matlab, to correct for incoherent averaging leading to artefactual signal loss. Eddy current correction was achieved using water reference. Spectra were analyzed with LCModel (21), using a basis set generated with home-made routines based on the density matrix formalism. Chemical shift and J-coupling values for metabolites were taken in Govindaraju et al (22). Signal could be reliably quantified according to our quality standards (Cramér-Rao lower bounds CRLB<5% at all *b*) for NAA, tCr, tCho, Ins, and Tau for all timing combinations. For the long TE experiments (TE = 73.4 ms, corresponding to four timing combinations), glutamate and glutamine could not be reliably quantified (CRLB > 5%) and are, therefore, not reported here.

Diffusion was analyzed by calculating the apparent diffusion coefficient (ADC) by log-linear regression up to $b = 5$ ms/μm^2, and also using biexponential fit up to $b = 30$ ms/μm^2, corresponding to the highest reachable *b*-value for the less favorable timing combinations. The stretched exponent (Kohlrausch–Williams–Watts relaxation functions) did not correctly fit the data at high *b*-values and was, therefore, not considered.

Statistical significance of the impact of TE and TM on signal attenuation or diffusion parameters was assessed by an analysis of variance (ANOVA) on two factors (TE and

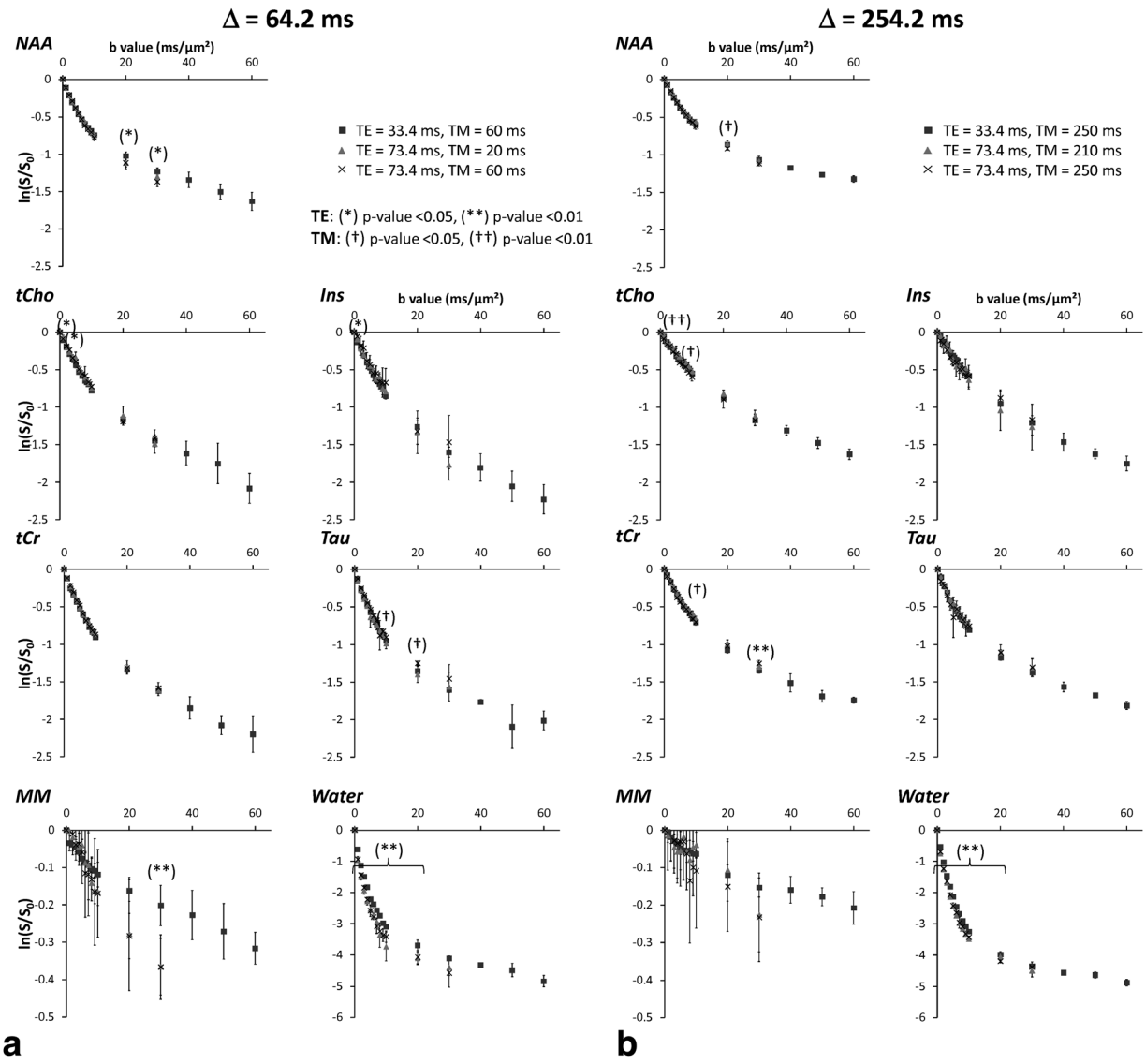

FIG. 5. A,B: Logarithm of signal attenuation for each metabolite and each TE/TM combination at the two different diffusion times, as a function of *b*. Error bars stand for the standard deviations determined on four mice. Asterisks indicate significant difference for different TE values: $^{*}P < 0.05$, $^{**}P < 0.01$. Daggers indicate significant difference for different TM values: $\dagger P < 0.05$, $\dagger\dagger P < 0.01$.

TM) for each metabolite at $\Delta = 64.2$ ms and $\Delta = 254.2$ ms, followed by a post hoc Tukey honest significant difference test on groups exhibiting significant differences extracted from the ANOVA (*P*-value < 0.05).

RESULTS

Effect of Varying TE and TM on Diffusion Attenuation

Representative spectra at all *b*-values and at all TE/TM/Δ combinations are shown in Figure 4. Note the very good SNR (SNR = 105 at $b = 0.050$ and SNR = 30 at $b = 60$ ms/μm^2 on the NAA peak on the most favorable timing combination, SNR = 78 at $b = 0.150$ and SNR = 27 at $b = 30$ ms/μm^2 on the less favorable timing combination). Logarithm of signal attenuation as a function of *b*, for each metabolite, is displayed on Figure 5A for $\Delta = 64.2$ ms, and of Figure 5B for $\Delta = 254.2$ ms. For each metabolite at each Δ, the three different TE/TM conditions are displayed on the same plot to facilitate comparison between these conditions.

Generally speaking, the impact of TE and TM is extremely low, whatever Δ. Only a few data points exhibit some significant dependency on TE/TM. Many of these data points are isolated, i.e., immediately lower and higher *b*-values do not exhibit any significant dependency on TE/TM, suggesting a possible type I error for at least some of these particular *b*-values for which dependency on TE/TM was identified. Anyway, for most of these *b*-values, signal difference between different TE/TM is less than 5%, which is in general below experimental noise and can, therefore, be considered negligible. The only exceptions are the dependency on TE of NAA attenuation at $b = 20$ ms/μm^2 and 30 ms/μm^2 (~7% signal decrease when increasing TE), and the dependency on TM of Tau attenuation at $b = 20$ ms/μm^2 (~13% when decreasing TM). To summarize, we can safely say

Table 1
Results from the Monoexponential and Biexponential Fits for Metabolites, MM, and Water Obtained under the Different TE/TM Combinations for $\Delta = 64.2$ ms[a]

	Δ=64.2 ms		Results from fit			
			Monoexponential	Biexponential		
	TE	TM	ADC	ADC_{fast}	ADC_{slow}	f_{slow}
NAA	33.4	60	0.097 ± 0.004	0.220 ± 0.023	0.019 ± 0.002	0.51 ± 0.03
	73.4	60	0.095 ± 0.004	0.181 ± 0.034	0.016 ± 0.010	0.44 ± 0.11
	73.4	20	0.094 ± 0.008	0.196 ± 0.029	0.021 ± 0.008	0.48 ± 0.11
tCr	33.4	60	0.109 ± 0.005	0.191 ± 0.033	0.023 ± 0.005	0.40 ± 0.09
	73.4	60	0.106 ± 0.005	0.204 ± 0.056	0.025 ± 0.009	0.43 ± 0.13
	73.4	20	0.101 ± 0.010	0.176 ± 0.041	0.019 ± 0.013	0.36 ± 0.12
tCho	33.4	60	0.091 ± 0.009	0.176 ± 0.011	0.024 ± 0.005	0.48 ± 0.06
	73.4	60	0.078 ± 0.008	0.184 ± 0.056	0.027 ± 0.009	0.52 ± 0.18
	73.4	20	0.082 ± 0.007	0.131 ± 0.035	0.012 ± 0.014	0.34 ± 0.14
Ins	33.4	60	0.098 ± 0.007	0.198 ± 0.034	0.029 ± 0.009	0.49 ± 0.12
	73.4	60	0.094 ± 0.005	0.283 ± 0.151	0.036 ± 0.025	0.59 ± 0.31
	73.4	20	0.086 ± 0.028	0.121 ± 0.006	0.010 ± 0.017	0.30 ± 0.15
Tau	33.4	60	0.118 ± 0.002	0.210 ± 0.033	0.022 ± 0.004	0.39 ± 0.06
	73.4	60	0.128 ± 0.016	0.220 ± 0.030	0.020 ± 0.016	0.38 ± 0.12
	73.4	20	0.112 ± 0.008	0.199 ± 0.033	0.014 ± 0.013	0.37 ± 0.09
MM	33.4	60	0.016 ± 0.005	0.861 ± 1.439	0.003 ± 0.003	0.89 ± 0.04
	73.4	60	0.011 ± 0.014	0.075 ± 0.071	0.010 ± 0.005	0.90 ± 0.05
	73.4	20	0.011 ± 0.007	0.053 ± 0.055	0.008 ± 0.006	0.88 ± 0.15
Water	33.4	60	0.491 ± 0.029 ***	0.649 ± 0.120	0.069 ± 0.028	0.09 ± 0.03*
	73.4	60	0.575 ± 0.010 ***	0.714 ± 0.113	0.048 ± 0.016	0.05 ± 0.02*
	73.4	20	0.568 ± 0.023 ***	0.735 ± 0.078	0.061 ± 0.017	0.06 ± 0.01*

[a]Units in the table are ms and μm^2/ms. Asterisks indicate significant difference for different TE values: *$P < 0.05$, **$P < 0.01$, ***$P < 0.005$, ****$P < 0.001$. Daggers indicate significant difference for different TM values: † $P < 0.05$. Statistical differences were evaluated using a one-way ANOVA test followed by *post hoc* analysis.

that, under the experimental conditions investigated here, the effect of TE and TM on metabolite diffusion attenuation is presumably very small (if any), with a possible but still ambiguous manifestation only at very high *b*-values in a limited number of cases.

We were also able to quantify MM signal attenuation, although quantification was relatively difficult for long TE. When looking at average MM signal, a consistently (i.e., for almost all *b*) stronger decrease is observed as TE is increased, although this decrease is not found to be significant, maybe due to the high measurement SD at long TE (type II error).

The situation is unambiguous for water, where a very significant ($P < 0.01$) dependency on TE is found at almost all *b*-values, for both Δ investigated: longer TE lead to stronger signal attenuation (no dependency on TM is found). This view is consistent with the existence of water pools with short T2/low diffusivity and long T2/fast diffusity, e.g., myelin water and cerebrospinal fluid.

Effect of Varying TE and TM on Estimated Diffusion Parameters

Table 1 and Table 2 summarize the estimated diffusion parameters derived from data for all metabolites in all conditions, respectively, for $\Delta = 64.2$ ms and $\Delta = 254.2$ ms. The variability for some parameters extracted from the biexponential fit is sometimes high, as expected when no a priori is used in the fitting. After ANOVA and post hoc analysis, no significant difference is found for any of the parameters under the various TE/TM combinations, whatever Δ or the metabolite considered. This confirms that the effect of TE and TM on metabolite measured diffusion is presumably very small, and maybe nonexistent. This is also true for MM, but the SD is very high, so here it is more difficult to rule out potential type II error. In contrast, diffusion parameters for water exhibit some very significant dependency on TE or TM.

DISCUSSION

Diffusion Properties of Metabolites in the Mouse Brain

Metabolite ADC measured here are in good agreement with measurements performed in the rat or monkey brain or in the human gray matter at intermediate/long diffusion times (higher than a few tens of ms) with state-of-the-art postprocessing (scan-to-scan phasing and MM quantification), i.e., in the order of 0.1–0.15 μm^2/ms [e.g., (6,7,20,23,24)]. Note that, in the present study, measured ADCs are generally in the lower range of (or slightly below) previously reported ADC. The linearity of signal logarithm attenuation in the $b = 0$–5 ms/μm^2 range is very good for all metabolites in all TE/TM/Δ conditions ($R^2 > 0.99$ in most situations, worst case for tCho at long TE where $R^2 = 0.96$, but SNR is lower).

In this work, we analyzed the diffusion properties in the range $b = 0$–30 ms/μm^2 using biexponential fitting. As far as we know, this can be compared with only one pioneering study where metabolite diffusion was measured

Table 2
Results from the Monoexponential and Biexponential Fits for Metabolites, MM, and Water Obtained under the Different TE/TM Combinations for $\Delta = 254.2$ ms[a]

	Δ=254.2 ms		Results from fit			
			Monoexponential	Biexponential		
	TE	TM	ADC	ADC_{fast}	ADC_{slow}	f_{slow}
NAA	33.4	250	0.077 ± 0.003	0.202 ± 0.027	0.018 ± 0.002	0.59 ± 0.04
	73.4	210	0.073 ± 0.004	0.202 ± 0.045	0.019 ± 0.005	0.61 ± 0.09
	73.4	250	0.076 ± 0.006	0.164 ± 0.019	0.016 ± 0.002	0.52 ± 0.02
tCr	33.4	250	0.083 ± 0.012	0.172 ± 0.044	0.022 ± 0.005	0.50 ± 0.08
	73.4	210	0.081 ± 0.007	0.213 ± 0.028	0.027 ± 0.004	0.63 ± 0.07
	73.4	250	0.089 ± 0.001	0.191 ± 0.029	0.020 ± 0.004	0.51 ± 0.06
tCho	33.4	250	0.063 ± 0.003	0.171 ± 0.046	0.025 ± 0.008	0.66 ± 0.12
	73.4	210	0.057 ± 0.011	0.168 ± 0.059	0.025 ± 0.008	0.70 ± 0.13
	73.4	250	0.062 ± 0.014	0.154 ± 0.067	0.017 ± 0.013	0.53 ± 0.22
Ins	33.4	250	0.063 ± 0.012	0.125 ± 0.051	0.013 ± 0.015	0.43 ± 0.20
	73.4	210	0.066 ± 0.018	0.111 ± 0.047	0.009 ± 0.009	0.34 ± 0.16
	73.4	250	0.081 ± 0.006	0.385 ± 0.333	0.024 ± 0.014	0.67 ± 0.17
Tau	33.4	250	0.101 ± 0.003	0.190 ± 0.030	0.018 ± 0.009	0.43 ± 0.09
	73.4	210	0.097 ± 0.005	0.222 ± 0.065	0.019 ± 0.014	0.49 ± 0.15
	73.4	250	0.122 ± 0.026	0.302 ± 0.068	0.025 ± 0.004	0.56 ± 0.04
MM	33.4	250	0.009 ± 0.003	0.291 ± 0.308	0.003 ± 0.002	0.90 ± 0.12
	73.4	210	0.012 ± 0.008	0.065 ± 0.117	0.006 ± 0.003	0.97 ± 0.04
	73.4	250	0.013 ± 0.014	0.122 ± 0.097	0.003 ± 0.003	0.89 ± 0.14
Water	33.4	250	0.453 ± 0.010****	0.523 ± 0.019****†	0.053 ± 0.006	0.059 ± 0.004
	73.4	210	0.529 ± 0.005****	0.637 ± 0.019****†	0.054 ± 0.008	0.055 ± 0.007
	73.4	250	0.520 ± 0.012****	0.603 ± 0.020****†	0.051 ± 0.005	0.051 ± 0.004

[a]Units in the table are ms and μm^2/ms. Asterisks indicate significant difference for different TE values: *$P < 0.05$, **$P < 0.01$, ***$P < 0.005$, ****$P < 0.001$. Daggers indicate significant difference for different TM values: † $P < 0.05$. Statistical differences were evaluated using a one-way ANOVA test followed by *post hoc* analysis.

up to $b = 49$ ms/μm^2 (at TE/TM/Δ = 22/111/122 ms) in the rat brain, and modeled by biexponential attenuation (20). Our own results are in rather good agreement with values reported in this past study for D_{fast} (~0.2–0.3 μm^2/ms), D_{slow} (~0.02–0.04 μm^2/ms), and f_{slow} (~50%). It can be noted that SD on estimated parameters, in particular f_{slow}, seems larger in our study, which we ascribe to the fact that here SD was determined from interindividual measurements and biexponential fits (which are known to be unstable), while in Pfeuffer et al (20), it was estimated by Monte Carlo simulation. We also used lower maximal *b*-values, because in the worst condition (long TE/TM experiments), we could not go higher than $b = 30$ ms/μm^2.

On the Absence of Dependency of Metabolite Diffusion on TE/TM

As far as we know, the dependency of diffusion properties on TM (at constant diffusion time) has never been studied. No dependency was found in the present work, but the range of TM explored here was very limited (compared with metabolite typical T1), because TM variation cannot be larger than 2τ (see Figure 2), and τ cannot be increased much if one wants to preserve high enough SNR on single scans. The possibility of a correlation between TM and T1 thus remains to be better characterized on a larger range of TM.

Three published works report some dependency of metabolite diffusion on TE (10–12). In the excised bovine optic nerve, Assaf and Cohen (11) report a strong effect of TE on tCho, tCr, and NAA diffusion (other metabolites were not measured), longer TE leading to more restricted apparent diffusion, for the investigated diffusion time Δ (95 ms). In the excised rat brain, the same group (10) reports an effect of TE on NAA diffusion (other metabolites were not measured), longer TE leading to larger fraction for the slow diffusing component, and in the meantime to larger D_{fast} and D_{slow}. In the human white matter, Branzoli et al (12) measured a complex dependency, with the ADC of NAA and tCr tending to increase with increasing TE for the short Δ condition (44 ms) tested, while the ADC of tCr tended to decrease with increasing TE for the long Δ condition (246 ms) tested, and no significant change was reported for tCho (other metabolites were not measured).

Methodological differences might partly explain the fact that, unlike here, these former studies detected some dependency on TE. In particular, in the works of Assaf and Cohen, it is not clear if scan-to-scan phasing was performed to correct for bulk translational motion. On the present data, absence of scan-to-scan phasing can lead to an overestimation of signal attenuation by a few tens of percent at high *b*, and bias of the same order of magnitude on diffusion parameters, illustrating the critical importance of performing scan-to-scan phasing. If different sequence timings resulted in different gradient and acoustic vibrations in these past works, translational motion may have been different for the different timings and have resulted in some bias, assuming no phase correction was performed. In addition, macromolecule signal was apparently not accounted for, while it can still be significant for TE shorter than 80–100 ms, even at

11.7 T. Finally, in the case of excised tissues, it is possible that homeostasis is not maintained anymore, leading to a "leakage" of metabolites into the extracellular space and a different diffusion-relaxation behavior.

A limitation of the present study is that the range of TE explored is narrower than in past studies, as we did not go to such long TE [up to 160 ms in the human brain (12), 200 ms in the rat brain (10) and 550 ms in the bovine optic nerve (11)]. This was dictated by the necessity to preserve high enough metabolite signal on individual scans to perform scan-to-scan phasing. The range of TE explored here would still be enough to significantly change the relative contribution of potential metabolic pools with "short" T2 [i.e., a few tens of ms, as identified in Assaf and Cohen (10,11)], thus allowing to detect potential different diffusion behavior of these short T2 pools compared with pools with longer T2. In that respect, we think that the narrower TE range is not likely to fully explain the discrepancy between our study and those having explored TE up to 200 ms in vivo (10,12). However, our study would not be very sensitive to detect potential correlation between diffusion and relaxation for the longer T2 pools (more than a few hundreds of ms), as identified in the excised optic nerve at TE = 550 ms (11).

Another potential explanation might be due to the different kinds of fibers investigated. While axons in the optic nerve and human white matter are myelinated, the total myelin content is low in the large voxel of the mouse brain investigated here, which contains a lot of gray matter. We actually evaluated the volume fraction occupied by white matter to be less than 20% in the spectroscopic voxel, based on fractional anisotropy maps that we acquired in some mice. Hence, a potential influence of myelin would be less diluted in (11,12) compared with the present study, possibly explaining a correlation due to myelin between TE and diffusion properties that we did not observe here. The source of such a "myelin effect" may be due to the presence of a metabolite compartment within the myelin sheath, but in that case, we rather expect this compartment to have a short T2 and highly restricted diffusion, which is not consistent with the studies of Assaf and Cohen and with the long Δ behavior in Branzoli et al. Another source of correlation might be the surface relaxivity of myelin, yielding an interplay between TE and measured diffusion properties that is certainly more complex, e.g., depending on the dispersity of geometries, but where stronger effects of surface relaxivity (e.g., at longer TE) might lead to an apparently more restricted diffusion (here we quote the words of Codd and Callaghan (25): "ignoring the presence of significant wall relaxation can lead to both an underestimation of the pore dimensions and a misidentification of the pore geometry").

A Few Words on Macromolecules

MM diffusion in the brain has received little attention to date. Pfeuffer et al (20) report an MM attenuation of 3% at $b = 5$ ms/μm^2 and TE/TM/Δ = 22/111/122 ms, which is of the same order of magnitude as what we measure here for the different timing combinations. They also report that MM attenuation is monoexponential up to $b = 49$ ms/μm^2 (although no figure displays MM attenuation and no R^2 is given), yielding an ADC of 0.0063 μm^2/ms, which is slightly lower than the values we report here when fitting in the $b = 0$–5 ms/μm^2 range (ADC$\sim$0.009–0.016 depending on the condition). If we perform a log-linear fit of the MM signal up to $b = 40$ (at $\Delta = 254.2$ ms) or 60 ms/μm^2 (at $\Delta = 64.2$ ms) for the "short TE" conditions (i.e., in the best SNR conditions for MM), we find ADC = 0.0103 or 0.0047 μm^2/ms, which is relatively similar to values reported in Pfeuffer et al (20). However, in the present work, we do not find a strictly monoexponential attenuation for MM, although the diffusion attenuation is indeed found to be much "less" biexponential than for metabolites, with a slow-diffusing fraction higher than $\sim$90% in all conditions.

Although the dependency of MM signal attenuation on TE is not significant according to ANOVA, the fact that the average attenuation is found consistently lower when TE is increased, for almost all *b*-values, suggests that a dependency on TE might indeed exist but be masked by measurement noise (type II error). We think this is plausible: one can indeed imagine a continuum of MM molecular weights contributing to MM signal (e.g., see Behar and Ogino) (26) with larger MM being associated with shorter T2 and slower diffusion. However, this remains to be confirmed by additional studies.

CONCLUSIONS

In this work, using a new sequence (dubbed "STE-LASER") yielding no cross-terms between selection and diffusion gradients, combined with state-of-the-art post-processing (including scan-to-scan phasing and experimental macromolecule signal quantification) and hardware (cryoprobe at 11.7 T) to minimize bias and maximize SNR, we measured little or no dependency of metabolite diffusion properties on TE/TM in a large voxel of the mouse brain in vivo, in the range of TE/TM values explored. These results are quite different from previous works, which might be due to methodological differences, and also to the different tissue composition of the voxels, in particular the relatively low amount of myelin in the large voxel of the present study. In our opinion, the present work strongly supports the practice of interpreting and modeling metabolite diffusion primarily based on geometry, irrespective of relaxation properties (multicompartmental relaxation or surface relaxivity), at least under the experimental conditions of this study. How to model these data will be the subject of future works. The potential correlation between macromolecule relaxation and diffusion, as well as the possible role of myelin in past studies reporting correlation between metabolites relaxation and diffusion, remain to be explored in deeper details.

ACKNOWLEDGMENTS

The 11.7 T MRI scanner was funded by a grant from "Investissements d'Avenir - ANR-11-INBS-0011" - NeurATRIS: A Translational Research Infrastructure for Biotherapies in Neurosciences.

REFERENCES

1. Nicolay K, Braun KP, Graaf RA, Dijkhuizen RM, Kruiskamp MJ. Diffusion NMR spectroscopy. NMR Biomed 2001;14:94–111.
2. Kroenke CD, Ackerman JJ, Yablonskiy DA. On the nature of the NAA diffusion attenuated MR signal in the central nervous system. Magn Reson Med 2004;52:1052–1059.
3. Marchadour C, Brouillet E, Hantraye P, Lebon V, Valette J. Anomalous diffusion of brain metabolites evidenced by diffusion-weighted magnetic resonance spectroscopy in vivo. J Cereb Blood Flow Metab 2012;32:2153–2160.
4. Ronen I, Ercan E, Webb A. Axonal and glial microstructural information obtained with diffusion-weighted magnetic resonance spectroscopy at 7T. Front Integr Neurosci 2013;7:13.
5. Ronen I, Budde M, Ercan E, Annese J, Techawiboonwong A, Webb A. Microstructural organization of axons in the human corpus callosum quantified by diffusion-weighted magnetic resonance spectroscopy of N-acetylaspartate and post-mortem histology. Brain Struct Funct 2014;219:1773–1785.
6. Najac C, Marchadour C, Guillermier M, Houitte D, Slavov V, Brouillet E, Hantraye P, Lebon V, Valette J. Intracellular metabolites in the primate brain are primarily localized in long fibers rather than in cell bodies, as shown by diffusion-weighted magnetic resonance spectroscopy. Neuroimage 2014;90:374–380.
7. Najac C, Branzoli F, Ronen I, Valette J. Brain intracellular metabolites are freely diffusing along cell fibers in grey and white matter, as measured by diffusion-weighted MR spectroscopy in the human brain at 7 T. Brain Struct Funct 2014. DOI: 10.1007/s00429-014-0968-5.
8. Mitra PP, Sen PN. Effects of microgeometry and surface relaxation on NMR pulsed-field-gradient experiments: simple pore geometries. Phys Rev B Condens Matter 1992;45:143–156.
9. Hurlimann MD, Latour LL, Sotak CH. Diffusion measurement in sandstone core: NMR determination of surface-to-volume ratio and surface relaxivity. Magn Reson Imaging 1994;12:325–327.
10. Assaf Y, Cohen Y. Non-mono-exponential attenuation of water and N-acetyl aspartate signals due to diffusion in brain tissue. J Magn Reson 1998;131:69–85.
11. Assaf Y, Cohen Y. Structural information in neuronal tissue as revealed by q-space diffusion NMR spectroscopy of metabolites in bovine optic nerve. NMR Biomed 1999;12:335–344.
12. Branzoli F, Ercan E, Webb A, Ronen I. The interaction between apparent diffusion coefficients and transverse relaxation rates of human brain metabolites and water studied by diffusion-weighted spectroscopy at 7 T. NMR Biomed 2014;27:495–506.
13. Does MD, Gore JC. Compartmental study of diffusion and relaxation measured in vivo in normal and ischemic rat brain and trigeminal nerve. Magn Reson Med 2000;43:837–844.
14. Le Bihan D, Joly O, Aso T, Uhrig L, Poupon C, Tani N, Iwamuro H, Urayama SI, Jarraya B. Brain tissue water comes in two pools: evidence from diffusion and R2' measurements with USPIOs in non human primates. Neuroimage 2012;62:9–16.
15. Shemesh N, Rosenberg JT, Dumez J-N, Muniz JA, Grant SC, Frydman L. Metabolic properties in stroked rats revealed by relaxation-enhanced magnetic resonance spectroscopy at ultrahigh fields. Nat Commun 2014;5:4958.
16. Garwood M, DelaBarre L. The return of the frequency sweep: designing adiabatic pulses for contemporary NMR. J Magn Reson 2001;153:155–177.
17. Valette J, Lethimonnier F, Lebon V. About the origins of NMR diffusion-weighting induced by frequency-swept pulses. J Magn Reson 2010;205:255–259.
18. Valette J, Giraudeau C, Marchadour C, Djemai B, Geffroy F, Ghaly MA, Le Bihan D, Hantraye P, Lebon V, Lethimonnier F. A new sequence for single-shot diffusion-weighted NMR spectroscopy by the trace of the diffusion tensor. Magn Reson Med 2012;68:1705–1712.
19. Kunz N, Cudalbu C, Mlynarik V, Huppi PS, Sizonenko SV, Gruetter R. Diffusion-weighted spectroscopy: a novel approach to determine macromolecule resonances in short-echo time 1H-MRS. Magn Reson Med 2010;64:939–946.
20. Pfeuffer J, Tkac I, Gruetter R. Extracellular-intracellular distribution of glucose and lactate in the rat brain assessed noninvasively by diffusion-weighted 1H nuclear magnetic resonance spectroscopy in vivo. J Cereb Blood Flow Metab 2000;20:736–746.
21. Provencher SW. Estimation of metabolite concentrations from localized in vivo proton NMR spectra. Magn Reson Med 1993;30:672–679.
22. Govindaraju V, Young K, Maudsley AA. Proton NMR chemical shifts and coupling constants for brain metabolites. NMR Biomed 2000;13:129–153.
23. Valette J, Guillermier M, Besret L, Boumezbeur F, Hantraye P, Lebon V. Optimized diffusion-weighted spectroscopy for measuring brain glutamate apparent diffusion coefficient on a whole-body MR system. NMR Biomed 2005;18:527–533.
24. Kan HE, Techawiboonwong A, van Osch MJ, Versluis MJ, Deelchand DK, Henry PG, Marjanska M, van Buchem MA, Webb AG, Ronen I. Differences in apparent diffusion coefficients of brain metabolites between grey and white matter in the human brain measured at 7 T. Magn Reson Med 2012;67:1203–1209.
25. Codd SL, Callaghan PT. Spin echo analysis of restricted diffusion under generalized gradient waveforms: planar, cylindrical, and spherical pores with wall relaxivity. J Magn Reson 1999;137:358–372.
26. Behar KL, Ogino T. Characterization of macromolecule resonances in the 1H NMR spectrum of rat brain. Magn Reson Med 1993;30:38–44.